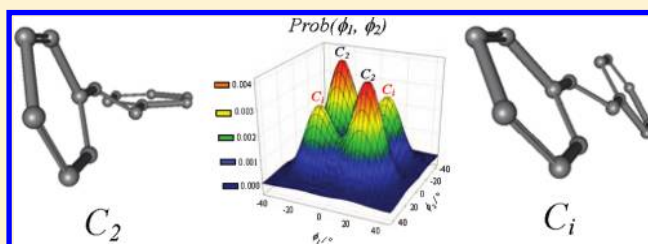


# Conformational Distribution of *trans*-Stilbene in Solution Investigated by Liquid Crystal NMR Spectroscopy and Compared with *in Vacuo* Theoretical Predictions

Giorgio Celebre,\* Giuseppina De Luca, and Maria Enrica Di Pietro

Dipartimento di Chimica, Università della Calabria, v. P. Bucci, I-87036 Rende (CS), Italy

**ABSTRACT:** The basic question about the structure and the conformational distribution of a  $\pi$ -conjugated, flexible organic molecule (interesting in itself, in relation to the balance of forces determining its torsional equilibrium) becomes a really intriguing problem in the case of *trans*-stilbene (*t*-St), a “fundamental” molecule from a chemical point of view, as well as the prototype fragment of a series of derivatives endowed with several important biological and technological properties. As a matter of fact, the problem of *t*-St planarity when the molecule is isolated or in solution is a particularly debated question. In the present paper we studied the conformational distribution of *t*-St in solution, by resorting to the powerful technique of liquid crystal NMR spectroscopy (LXNMR), and we compared the obtained experimental results with accurate theoretical calculations carried out *in vacuo*, by using the MP2/6-31G\*\* method (allowing for bond lengths and angles relaxation every 3° torsional steps). Our theoretical and experimental outcomes agree in indicating the nonplanarity of the molecule which, on the contrary, exhibits the coexistence of four stable rotamers, two by two symmetry related. In particular, we have found a couple of global minima corresponding to propeller-like  $C_2$  symmetry conformations, where both the rings are “disrotated”, with respect to the vinyl group, of about 17° in solution and of 27° *in vacuo* (theoretical value). Besides this, the presence of a couple of  $C_i$  local minima, with both the rings “conrotated” of 17° (fluid phase) or of 27° (MP2/6-31G\*\* calculations for the isolated molecule) has been determined.



## 1. INTRODUCTION

The structure and conformational distribution of *trans*-diphenylethene, better known as *trans*-stilbene (*t*-St) and representing the shortest oligomer of the poly(*p*-phenylenevinylene) family, has attracted much interest over the last decades. The structures and the point groups of those that, presumably, represent the three most probable candidates to be stable conformations for *t*-St are described in Figure 1 (where also the sign convention for internal rotations is shown):  $C_{2h}$  (full planar molecule),  $C_2$  (disrotatory, propeller-like conformation, where the rings are tilted at the same angle with respect to the *ene* plane, i.e.  $\phi_1 = \phi_2$ ) and  $C_i$  (conrotatory conformation, where the rings are parallel to each other, i.e. tilted at angles equal in magnitude but opposite in sign:  $\phi_1 = -\phi_2$ ). The question about the planarity of a  $\pi$ -conjugated organic molecule is interesting in itself, in relation to the balance of forces determining its conformational equilibrium. In the particular case of *t*-St, the torsional distribution is, of course, the result of the balance between the steric repulsions of the phenyl groups and the vinyl system and the loss in conjugation energy stabilization of the just cited  $\pi$  systems. Anyway, besides the fundamental interest for structural and conformational determinations, there is also another reason why, in our opinion, the *t*-St conformational equilibrium deserves to be studied. As a matter of fact, this molecule and its derivatives show several interesting biological and technological properties

that could be affected, to a certain extent, by the rotameric distribution of the molecule.

About the biochemistry of the molecule, many naturally occurring stilbenic compounds, namely resveratrol (3,4',5-trihydroxy-*trans*-stilbene), piceatannol (3,3',4',5-tetrahydroxy-*trans*-stilbene) or rhapontigenin (3,3',5-trihydroxy-4'-methoxy-*trans*-stilbene), have been reported to possess multiple healthy biological activities.<sup>1</sup> As a consequence, the last decades have witnessed intense research devoted to these natural compounds and their analogues, that can play an important role in the prevention of a wide variety of human pathological processes.<sup>1a,b,2–6</sup> Moreover, green plants of various taxonomic groups naturally biosynthesize stilbenoid compounds acting as protective agents against adverse conditions, such as microbial attacks or environmental stress.<sup>7</sup> If, on the contrary, we consider the technological point of view, it is well known that *t*-St is the building block of several commercially available liquid crystals and it has been included in many macromolecular backbones, such as polymers or dendrimers, for inducing liquid-crystalline behavior.<sup>8</sup> More, conjugated polymers, such as poly(*p*-phenylenevinylene), present semiconducting characteristics, are optically active in the visible region, and

**Received:** December 12, 2011

**Revised:** February 9, 2012

**Published:** February 9, 2012

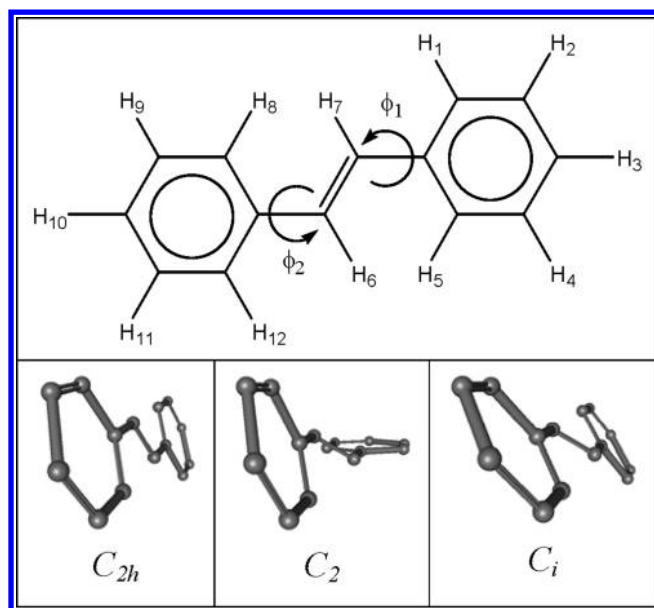


**Figure 1.** *trans*-Stilbene: hydrogen numbering, torsional angles  $\phi_1$  and  $\phi_2$  and possible stable structures (with corresponding point groups).

at the same time promise mechanical flexibility, ease and, consequently, low cost of fabrication through wet chemistry, motivating thus intensive research worldwide.<sup>9</sup> Stilbene and its related substituted analogues are also associated with photochemical and photophysical phenomena and are among the most widely investigated organic chromophores.<sup>10</sup> Photosystems including stilbenic molecules are used in LEDs, photoresistors, photoconductive devices, imaging and optical switching techniques, materials for nonlinear optics (NLO) and laser dyes.<sup>11</sup> Finally, stilbene moieties have been used as photoresponsive groups to functionalize different kinds of devices such as hydrogels or polymeric vesicles, making them susceptible to light stimuli for a photochemical control of drug release.<sup>12</sup> As said above, all these properties could depend (totally or, at least, in part) on the molecular conformations, and in fact the problem of *t*-St planarity is a particularly debated question.<sup>13–38</sup> It is worth emphasizing that the conformational equilibrium of *t*-St is, in principle, affected by the material's phase. This means that the molecule could show different torsional distributions depending on its physical state and, as a matter of fact, it has been found to be basically planar in solid phase<sup>13,14</sup> (the greatest deviation from planarity being a twist angle of 5° of the phenyl from the vinyl group<sup>13</sup>). The *t*-St rotameric equilibrium has been also investigated in polycrystalline *n*-alkane lattices at very low temperatures, by the so-called Shpolskii spectroscopy (see 15 and references therein). The resolved absorption, fluorescence excitation and fluorescence spectra of *t*-St in *n*-C<sub>6</sub> and *n*-C<sub>8</sub> matrices at 5 K led the authors to assess that the *t*-St molecule tends to be, at most, just slightly twisted, so that its symmetry is either C<sub>2h</sub> or C<sub>i</sub>, as in the pure crystal.<sup>15</sup> When, on the contrary, we pass to consider the results in vapor phase, we discover that they are quite controversial. Optical absorption,<sup>16</sup> two-color stimulated emission spectroscopy,<sup>17</sup> pure rotational coherence effects on picosecond fluorescence polarization experiments<sup>18</sup> and

several other fluorescence studies<sup>19–23</sup> seem to lead to a C<sub>i</sub> or a C<sub>2h</sub> planar structure for the isolated molecule. Anyway, other fluorescence works disagree with these outcomes, suggesting that the structure for the molecule is basically C<sub>2</sub>.<sup>24</sup> This is in agreement with gas electron diffraction results, that gives a C<sub>2</sub> structure where the rings are rotated of 32.5°. <sup>25</sup> Photoelectron spectroscopy also has yielded conflicting results: a quite old study found a planar structure,<sup>26</sup> whereas a more recent work concludes that the phenyl groups are twisted of about 15–20°. <sup>27</sup> From a theoretical point of view, calculations for the isolated molecule (*in vacuo*) give different results depending on the used methods and basis sets: B3LYP/6-31G, and B3LYP/6-31G\*\* found that the molecule is planar; on the contrary, the studies carried out by using HF/6-31G, HF/6-31G\*\* and MP2/6-31G\*\* gave the *t*-St to be nonplanar.<sup>28</sup> About this, an high level theoretical study of the structure and rotational barriers of *t*-St<sup>29</sup> emphasizes that the controversy is still unresolved. As a matter of fact, DFT functionals (producing the planar result, as said above) are believed to fail in correctly describing long-range nonbonding interactions, whereas several other methods (widely tested and illustrated in that paper,<sup>29</sup> by investigating also the basis set dependence of the results) contrast with the benchmark calculations there presented (MP2 geometry optimization using the aug-cc-pVDZ basis set). This leads the authors to the conclusion that, in the non relativistic limit and within the frozen core approximation, *t*-St *in vacuo* is a strictly planar molecule in its absolute energy minimum form. Other authors obtain that the ground-state equilibrium geometry of Stilbene in its *trans* conformation, optimized at the SA-2-CAS(2/2) level, is a nonplanar, approximately C<sub>2v</sub> symmetry structure,<sup>30</sup> whereas fully relaxed *ab initio* RHF/3-21G calculations (preliminary to the introduction of correlation effects, included by using B3LYP functional and 6-31G(d) basis set)<sup>31</sup> interestingly show four (two global and two local) symmetry related torsional minima. In the two absolute minima, the planes of the phenyl groups are tilted in a non-parallel, C<sub>2</sub> symmetry way (so that the authors call them **np**), with the dihedral angles between the rings and the ethylenic group of 27° (or 23°, depending on the used basis set); on the contrary, in the relative minima (C<sub>i</sub> structures called **p**) the phenyls are parallel and tilted of the same angle of 27° (or 23°) magnitude. Semiempirical methods PM5 and AM1 predict a nonplanar ground state for *t*-St, while PM3 predicts the planar one.<sup>32</sup> Intriguingly, there is also a study suggesting that *t*-St is planar at low temperature in gas phase, but departs from planarity as the temperature is raised.<sup>33</sup> Another theoretical study suggests possible important effects of the zero point vibrational energy (ZPVE) correction, in the adiabatic approximation, on the torsional barrier of *t*-St: ZPVE corrections could play a significant role in the experimentally observed planar structure of the molecule.<sup>34</sup> A predominant C<sub>2</sub> structure for the molecule is also found by Raman spectroscopy in fluid phases (in the melt and in solution).<sup>35</sup> NMR techniques in isotropic phase confirm the twisted nature of *t*-St in solution, by studying the conformational dependence of deuterium-induced isotopic effects.<sup>36</sup> Contrary to what just said, another study, aimed to obtain conformational information on *t*-St in solution from vibrational spectra, leads to the result that the molecule is planar in solution,<sup>37</sup> implying

that this preferred molecular conformation is mainly determined by intermolecular rather than intramolecular forces. Finally, other authors<sup>38</sup> observe that the Raman spectrum of *t*-St in solution shows a weak band at about 960 cm<sup>-1</sup> (due to the in-phase ethylenic CH wag), which is not present in the solid state. Now, the in-phase ethylenic CH wag is Raman-inactive for the planar structure and acquires higher Raman intensities with increasing degree of molecular distortion. From these premises, the conclusions of the paper are that the probable range of torsional distortion around the C=C bond is 2.5–4.0° while the tilt angle from the planar structure is 8.0–12.0° around the C–Ph bond.<sup>38</sup> About the reasons why the molecule in solution is distorted from the planar structure, the authors say that no simple answers to this question are available: solvation, dimerization, clustering, etc., occurring in solution or in the liquid state may account for the stabilization of the system accompanied by molecular distortion, but no evidence for any of such possibilities has been obtained. In this work, we will present the results obtained about the *t*-St conformational distribution in solution, studied by the powerful technique of liquid crystal NMR spectroscopy (LXNMR),<sup>39–46</sup> (there is also an Appendix at the end of the paper) and we will compare the obtained experimental results with accurate theoretical calculations for the isolated molecule.

## 2. THEORETICAL BACKGROUND OF THE LXNMR APPROACH

The target of our LXNMR spectral analysis (described in the next section) is represented by the observed  $D_{ij}^{obs}$  dipolar (or direct) couplings between the *i*th and *j*th magnetically active nuclei present in the studied molecule (in this case, the protons of *t*-St). The observed dipolar couplings are partially averaged quantities, where the average is over all the relevant motions of the molecule (namely, internal vibrations and rotations and whole reorientational motions, often called “overall rotations” or “molecular tumbling”) with respect to the external applied magnetic field  $B_0$ , conventionally aligned along the *Z* direction of the Laboratory reference system (so that, in practice,  $D_{ij}^{obs} \equiv \tilde{D}_{ijZZ}$ , where the tilde symbol “~” represents the process of average). Given the aim and the nature of the present work, involving only interproton dipolar couplings, the approximation of neglecting the effects of high-frequency, small-amplitude molecular vibrations can be quite safely adopted (for detailed information about vibrational corrections in LXNMR and their importance in structural-conformational determinations, the reader is referred to refs 43–48 and references therein). Moreover, for small flexible molecules with two internal rotational degrees of freedom  $\phi_1$  and  $\phi_2$  (as is the case of *t*-St; see Figure 1) undergoing large-amplitude motions which are fast compared with the changes produced in the couplings, the internal motion can be explicitly taken into account by its torsional probability distribution  $p(\phi_1, \phi_2)$ . In the light of the above considerations, it can be shown that the

observed dipolar couplings can be quite properly approximated by the following formula:<sup>44a</sup>

$$D_{ij}^{obs} \equiv \tilde{D}_{ijZZ} \approx \left( \frac{3 \cos^2 \alpha - 1}{2} \right) \times \frac{2}{3} \int_{\phi_2} \int_{\phi_1} \int_{\gamma} p_{LC}(\beta, \gamma, \phi_1, \phi_2) \times \sum_{\rho\sigma} ((3[\cos \omega_\rho]_{(\beta,\gamma)}[\cos \omega_\sigma]_{(\beta,\gamma)} - \delta_{\rho\sigma})/2) \times D_{ij}^{\rho\sigma}(\phi_1, \phi_2) \sin \beta \, d\beta \, d\gamma \, d\phi_1 \, d\phi_2 = \left( \frac{3 \cos^2 \alpha - 1}{2} \right) \left[ \frac{2Z_{iso}}{3Z} \int_{\phi_2} \int_{\phi_1} p_{iso}(\phi_1, \phi_2) \times W(\phi_1, \phi_2) \sum_{\rho\sigma} S_{\rho\sigma}(\phi_1, \phi_2) \times D_{ij}^{\rho\sigma}(\phi_1, \phi_2) \, d\phi_1 \, d\phi_2 \right] \quad (1)$$

where  $\alpha$  is the angle between  $B_0$ , defining the *Z* direction in the laboratory frame, and  $\hat{n}$ , the director of the mesophase;<sup>44b</sup> the Euler angles  $\{\beta, \gamma\}$  characterize the orientation of  $\hat{n}$  in the molecule-fixed frame and  $\omega_\rho$  (which is a function of  $\beta$  and  $\gamma$ ) is the instantaneous angle between  $\hat{n}$  and the  $\rho$  axis of a Cartesian coordinate system fixed on the solute molecule;  $\delta_{\rho\sigma}$ , finally, is the Kronecker delta function. The terms (a)  $S_{\rho\sigma}(\phi_1, \phi_2)$  (called “order parameters”) and (b)  $D_{ij}^{\rho\sigma}(\phi_1, \phi_2)$  are, respectively: (a) the Cartesian components, given in the molecular frame, of the Saupe matrix *S* (describing the orientational ordering of the solute, i.e., the degree of statistical alignment of the molecular axes to the director) and (b) the Cartesian components, given in the molecular frame, of the  $D_{ij}$  tensor of the dipolar coupling between the *i*th and *j*th nucleus. Both depend on the molecular conformation, defined by the torsional angles  $\phi_1$  and  $\phi_2$ . About the  $D_{ij}$  tensor, the following relation holds:

$$D_{ij}^{\rho\sigma}(\phi_1, \phi_2) = -\frac{K_{ij}}{r_{ij}^3(\phi_1, \phi_2)} \times [3 \cos \vartheta_{ij}^\rho(\phi_1, \phi_2) \times \cos \vartheta_{ij}^\sigma(\phi_1, \phi_2) - \delta_{\rho\sigma}] \quad (2)$$

with

$$K_{ij} = \frac{\mu_0 \hbar \gamma_i \gamma_j}{16\pi^2} \quad (3)$$

$\gamma_i$  and  $\mu_0$  being respectively the *i*th nuclear magnetogyric ratio and the vacuum magnetic permeability, and  $\vartheta_{ij}^\rho$  the angle between the distance vector  $\mathbf{r}_{ij}$  and the  $\rho$  molecular axis. With regard to the order parameters, they can be written as:

$$S_{\rho\sigma}(\phi_1, \phi_2) = \left[ \int ((3[\cos \omega_\rho]_{(\beta,\gamma)}[\cos \omega_\sigma]_{(\beta,\gamma)} - \delta_{\rho\sigma})/2) \times p_\Omega(\beta, \gamma, \phi_1, \phi_2) \sin \beta \, d\beta \, d\gamma \right] / \left[ \int p_\Omega(\beta, \gamma, \phi_1, \phi_2) \, d\beta \, d\gamma \right] \quad (4)$$

A thorough examination of eq 1 leads to conclude that the term  $p_{LC}(\beta, \gamma, \phi_1, \phi_2)$  (giving the probability of finding the mesophase director  $(\beta, \gamma)$ -oriented in the solute-fixed frame,



when the probe-molecule is in its  $\{\phi_1, \phi_2\}$  conformation in the liquid crystalline solution) is necessarily the following:

$$p_{LC}(\beta, \gamma, \phi_1, \phi_2) = \frac{p_{\Omega}(\beta, \gamma, \phi_1, \phi_2) p_{iso}(\phi_1, \phi_2) W(\phi_1, \phi_2) Z_{iso}}{Z} \quad (5)$$

being the following relations verified in eqs 1 and 4:

$$Z_{iso} = \int p_{iso}(\phi_1, \phi_2) d\phi_1 d\phi_2 \quad (6)$$

$$Z = \int W(\phi_1, \phi_2) p_{iso}(\phi_1, \phi_2) d\phi_1 d\phi_2 \quad (7)$$

$$W(\phi_1, \phi_2) = \int \exp[-U_{ext}(\beta, \gamma, \phi_1, \phi_2)/k_B T] \times \sin \beta d\beta d\gamma \quad (8)$$

$$p_{\Omega}(\beta, \gamma, \phi_1, \phi_2) = \frac{\exp[-U_{ext}(\beta, \gamma, \phi_1, \phi_2)/k_B T]}{Q} \quad (9)$$

with

$$Q = \int \exp[-U_{ext}(\beta, \gamma, \phi_1, \phi_2)/k_B T] \times \sin \beta d\beta d\gamma d\phi_1 d\phi_2 \quad (10)$$

where  $k_B$  is the Boltzmann constant and  $U_{ext}(\beta, \gamma, \phi_1, \phi_2)$  is a solute–solvent purely anisotropic external orientational potential. Very importantly,  $p_{iso}(\phi_1, \phi_2)$  of eqs 1 and 5 represents the probability distribution of the solute in a “virtual” isotropic phase of the nematic solvent at the experiment temperature: it is, after all, the basic target of conformational studies in liquids.<sup>44a</sup> In order to calculate the order parameters  $S_{\rho\sigma}(\phi_1, \phi_2)$  of eqs 1 and 4, it is necessary to adopt a theoretical model describing the interdependent conformational-orientational problem. Here, we used the AP-DPD approach (additive potential<sup>45,46</sup> for the treatment of the ordering interactions, combined with the direct probability description of the torsional distribution  $p_{iso}(\phi_1, \phi_2)$ ).<sup>41,47–54</sup> In the particular case of *t*-St, the  $p_{iso}(\phi_1, \phi_2)$  has been modeled directly as a sum of bidimensional Gaussian functions:

$$p_{iso}(\phi_1, \phi_2) \propto \frac{w(C_2)}{4} (e^{-(\sin^2(\phi_1 - \phi_1^M)/2h_1^2) + (\sin^2(\phi_2 - \phi_2^M)/2h_2^2)} + e^{-(\sin^2(\phi_1 - (\pi - \phi_1^M))/2h_1^2) + (\sin^2(\phi_2 - (\pi - \phi_2^M))/2h_2^2)} + e^{-(\sin^2(\phi_1 - (\pi - \phi_1^M))/2h_1^2) + (\sin^2(\phi_2 + \phi_2^M)/2h_2^2)} + e^{-(\sin^2(\phi_1 - \phi_1^M)/2h_1^2) + (\sin^2(\phi_2 + (\pi - \phi_2^M))/2h_2^2)}) + \frac{w(C_i)}{4} (e^{-(\sin^2(\phi_1 - \phi_1^M)/2h_1^2) + (\sin^2(\phi_2 + \phi_2^M)/2h_2^2)} + e^{-(\sin^2(\phi_1 - (\pi - \phi_1^M))/2h_1^2) + (\sin^2(\phi_2 + (\pi - \phi_2^M))/2h_2^2)} + e^{-(\sin^2(\phi_1 - (\pi - \phi_1^M))/2h_1^2) + (\sin^2(\phi_2 - \phi_2^M)/2h_2^2)} + e^{-(\sin^2(\phi_1 - \phi_1^M)/2h_1^2) + (\sin^2(\phi_2 - (\pi - \phi_2^M))/2h_2^2)}) \quad (11)$$

where  $\phi_1^M$  and  $\phi_2^M$  represent the most probable values of the twist angles shown in Figure 1;  $w_{(C_2)}$  and  $w_{(C_i)}$  are the relative weights of the  $C_2$  and  $C_i$  structures (we also fixed the constraint that  $w_{(C_2)} + w_{(C_i)} = 1$ ) and, finally,  $h_1$  and  $h_2$  give the width at

half-maximum height along each dimension of the bidimensional Gaussians (note that the use of sinusoidal functions in the exponent of the Gaussians, introduced by us for the first time with this work, assures the right periodicity of the  $p_{iso}$  probability distribution simplifying its analytical expression with respect to those used in the past papers).<sup>41,47–54</sup> About the term  $U_{ext}(\beta, \gamma, \phi_1, \phi_2)$  of eqs 8–10, it is described as follows:

$$U_{ext}(\beta, \gamma, \phi_1, \phi_2) = -\varepsilon_{2,0}(\phi_1, \phi_2) C_{2,0}(\beta) - 2 \operatorname{Re}(\varepsilon_{2,2}(\phi_1, \phi_2)) \operatorname{Re}(C_{2,2}(\beta, \gamma)) \quad (12)$$

Here the  $C_{2,m}(\beta, \gamma)$  are modified spherical harmonics,<sup>55</sup> and the  $\varepsilon_{2,m}(\phi_1, \phi_2)$  are the elements of suitable conformation-dependent solute–solvent interaction tensors. The peculiar feature of the AP method is that the general  $\varepsilon_{2,m}(\{\phi\})$  elements are constructed as a sum of conformationally independent terms  $\varepsilon_{2,p}(l)$  representing the single contributions of each rigid fragment  $l$  in the molecule to the whole interaction tensors:

$$\varepsilon_{2,m}(\{\phi\}) = \sum_l \sum_p \varepsilon_{2,p}(l) D_{p,m}^2(\Lambda_{\phi}^l) \quad (13)$$

(in eq 13, the second-rank Wigner rotation matrix  $D_{p,m}^2(\Lambda_{\phi}^l)$ <sup>55</sup> relates the conformation-dependent  $\Lambda_{\phi}^l$  orientation of the  $l$ th molecular subunit to the molecule-fixed reference frame). Essentially, the  $\varepsilon_{2,p}(l)$  are unknown quantities whose values are adjusted to produce the best agreement with the experimental data. Once they are known, following the equations given above, it is possible to predict the behavior of the order parameters as a function of the molecular conformation. The use of all this theoretical apparatus will be described “in action” in the section 4 (Conformational Analysis by LXNMR).

### 3. PREPARATION OF THE SAMPLE, NMR EXPERIMENT, AND ANALYSIS OF <sup>1</sup>H-LXNMR SPECTRUM

In order to obtain the experimental data set of interproton observed dipolar couplings  $D_{ij}^{obs}$ , a dilute solution (approximately 5 wt %) was prepared by dissolving the *t*-St molecule (available from Aldrich) in a commercial nematic solvent (from Merck), known as ZLI1132 (a mixture of three phenyl cyclohexanes and one biphenyl cyclohexane; more information about the chemical nature of ZLI1132 can be found, for example, in ref 41). The sample was heated a few times up to its nematic–isotropic transition temperature  $T_{NI}$  and strongly shaken to homogenize the solution; then, it has been left to cool slowly in the magnetic field of the NMR spectrometer. The <sup>1</sup>H-LXNMR spectrum was recorded at room temperature (298 K) on a Bruker Avance 500 MHz (11.74 T) instrument. The extremely complex proton spectrum, shown in Figure 2 (being the molecule, from a NMR point of view, a 12-spin system, the spectrum is affected by a good 19 independent dipolar coupling constants  $D_{ij}^{ph}$ ), was analyzed by using a homemade, user-assisted iterative computer program called ARCANA.<sup>42</sup>

The first step of the analysis of such a crowded spectrum requires a quite reliable estimation of the spectral parameters, in order to calculate a sufficiently good starting trial spectrum. The starting values of chemical shifts  $\delta_{ij}$  and scalar couplings  $J_{ij}$  were taken from the routine analysis of the proton NMR spectrum of a isotropic solution of *t*-St dissolved in CDCl<sub>3</sub>; moreover, looking for a starting set of dipolar couplings good enough to reproduce at

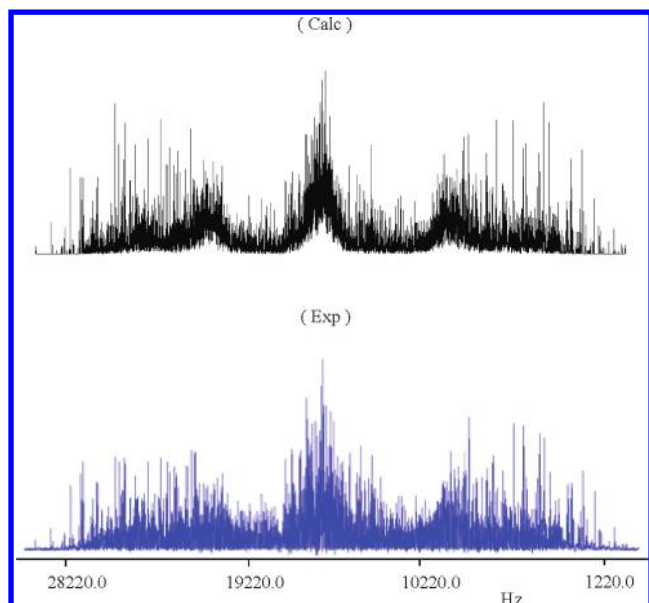


**Figure 2.** The 500 MHz  $^1\text{H}$ -LXNMR experimental spectrum (bottom, in blue) of *trans*-stilbene dissolved in the liquid crystalline nematic mesophase ZLI1132 at 298 K. For comparison, the spectrum calculated by using the  $D_{ij}^{\text{obs}}$  spectral parameters (obtained from the analysis and reported in Table 1) is also shown, in black, at the top of the figure.

best (or, at least, in an acceptable way) the basic features of the spectrum, two different trial sets of  $D_{ij}^{\text{trial}}$  were produced by fixing the geometry of the molecule in both planar,  $C_{2h}$  symmetry, and nonplanar,  $C_2$  symmetry, structure (see Figure 1). The  $D_{ij}^{\text{trial}}$  obtained by fixing the molecule in the planar conformation and adjusting, by trial and error, the longitudinal order parameter  $S_{cc}$  and the biaxiality order parameter  $S_{aa} - S_{bb}$  (see Figure 3 for the

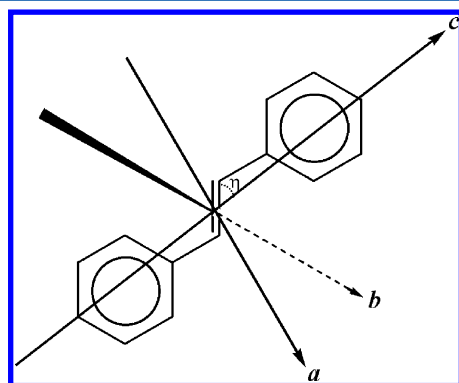


**Figure 3.** Definition of the  $\{a, b, c\}$  molecular frame for *trans*-stilbene (the  $b$  axis is perpendicular to the  $(ac)$  plane, where the vinyl group lies). Moreover, in the figure is also shown the  $\eta$  angle (describing an integral rotation of the  $\{a, b, c\}$  system about the  $b$  axis) which locates the Principal axis system (PAS) of the  $S$  matrix for the  $C_2$  structure (see the section 4 for details).

definition of the  $\{a, b, c\}$  molecular frame) were rejected because we immediately realized that the simulated trial spectra (corresponding to different sets of  $D_{ij}^{\text{trial}}$  obtained as functions of the  $S_{ij}$  variables) invariably showed a distribution of lines completely incompatible with the experimental one.

This was the first significant, “model-free” symptom we recorded where the molecule is not planar in solution (this point will be taken up in the discussion of section 6). On the contrary, a reasonable set of starting dipolar couplings was

predicted by guessing from literature<sup>27</sup> a nonplanar conformation with a torsion angle  $\phi_1 = \phi_2$  of about  $15^\circ$  and two trial order parameters having the values  $S_{cc} = 0.590$  and  $S_{aa} - S_{bb} = 0.134$ . In this case, the trial spectrum was sufficiently close, in terms of total width and line distribution, to the observed one and this led us to the successful analysis. The whole set of final spectral parameters is reported in Table 1.

**Table 1.** Chemical Shifts  $\delta_{ij} = \nu_i - \nu_j$ , Scalar Couplings  $J_{ij}$ , and Observed Dipolar Couplings  $D_{ij}^{\text{obs}}$  ( $i$  and  $j$  Hydrogen Labels from Figure 1) Determined by the Analysis of  $^1\text{H}$ -LXNMR Spectrum of *trans*-Stilbene Dissolved in ZLI1132<sup>a</sup>

$ij$	$J_{ij}/\text{Hz}$	$D_{ij}^{\text{obs}}/\text{Hz}$	$D_{ij}^{\text{AP-DPD}}/\text{Hz}$
1,2	8.00	$-4004.33 \pm 0.03$	$-4004.85$
1,3	2.00	$-507.48 \pm 0.06$	$-507.37$
1,4		$-1.48 \pm 0.04$	$-0.69$
1,5	2.00	$247.46 \pm 0.08$	$246.73$
1,6		$-2462.52 \pm 0.08$	$-2462.51$
1,7		$-1732.91 \pm 0.07$	$-1732.84$
1,8		$-397.17 \pm 0.05$	$-399.16$
1,9		$-140.41 \pm 0.04$	$-138.98$
1,10		$-104.60 \pm 0.06$	$-103.64$
2,3	6.00	$-20.45 \pm 0.06$	$-19.85$
2,4	2.00	$246.98 \pm 0.08$	$248.33$
2,6		$-380.11 \pm 0.09$	$-376.75$
2,7		$-364.85 \pm 0.09$	$-364.74$
2,9		$-64.74 \pm 0.06$	$-63.36$
2,10		$-50.75 \pm 0.06$	$-49.68$
3,6		$-254.36 \pm 0.14$	$-256.08$
3,7		$-271.60 \pm 0.14$	$-270.23$
3,10		$-39.58 \pm 0.08$	$-39.82$
6,7	17.50	$681.36 \pm 0.10$	$676.55$
$ij$	$\delta_{ij}/\text{Hz}$		
15,17	$-459.39 \pm 0.06$		
16,17	$-444.85 \pm 0.07$		
25,17	$-666.61 \pm 0.07$		

rms = 1.67 Hz

<sup>a</sup>In the last column, the  $D_{ij}^{\text{AP-DPD}}$  values, obtained from the so-called AP-DPD method (see Sections 2 and 4, for the description of the model and its application), are also reported for comparison. Finally, in order to emphasize the good performance of the used approach, the resulting value of RMS (the root mean square target function) between AP-DPD-calculated and observed dipolar coupling values is reported in the last row.

#### 4. CONFORMATIONAL ANALYSIS BY LXNMR

Following the theoretical background and the approximations described in section 2, it is possible to realize immediately that, for the case studied in the present work, the observed dipolar couplings of eq 1 can be effectively rewritten as:

$$D_{ij}^{\text{obs}} = \frac{2Z_{\text{iso}}}{3Z} \int_{\phi_2} \int_{\phi_1} p_{\text{iso}}(\phi_1, \phi_2) W(\phi_1, \phi_2) \times \sum_{\rho\sigma} S_{\rho\sigma}(\phi_1, \phi_2) D_{ij}^{\rho\sigma}(\phi_1, \phi_2) d\phi_1 d\phi_2 \quad (15)$$

As said above, the distinctive feature of eq 15, making the LXNMR technique so useful for studying the conformations of flexible molecules in solution, is the presence in the formula of the  $p_{\text{iso}}$  function: this can allow for the determination of the conformational probability from the experimental dipolar

couplings. It is worthwhile to emphasize that  $p_{iso}$  should be considered, in principle, as the “real” conformational distribution of our solute in a “conventional” isotropic liquid sharing, at the studied temperature, the same physical properties (determining the thermodynamics of the solution, as, for example, polarity, density etc.) of the used liquid crystalline solvent, with the exception of its ordering power (in other words, unlike the  $p_{LC}(\phi_1, \phi_2)$  of eqs 1 and 5,  $p_{iso}(\phi_1, \phi_2)$  is in principle free from possible conformational effects induced by the orientational ordering of the mesophase). In the light of sections 2 and 3, we think it can now be useful to quickly summarize the basic steps leading to the LXNMR determination of the conformational distribution of the studied molecule as well as of its orientational behavior: 1) the direct couplings  $D_{ij}^{obs}$  are obtained from the analysis of the  $^1\text{H}$ -LXNMR spectrum; 2) the dipolar coupling tensor  $D_{ij}^{p\sigma}(\phi_1, \phi_2)$ , for each  $(\phi_1, \phi_2)$  conformation and for each  $i$ - $j$  pair of hydrogens, is obtainable on the basis of the molecular geometry; the interdependent 3) conformation-dependent Saupe matrix  $S_{p\sigma}(\phi_1, \phi_2)$  and 4) torsional distribution  $p_{iso}(\phi_1, \phi_2)$ , are derived from a fit of the experimental data set of point 1), by assuming a model (in our case, the AP-DPD) for their dependence upon the  $\{\phi_1, \phi_2\}$  angles. In treating the  $t$ -St molecule we assumed, as usually done in literature,<sup>44a,48</sup> that the phenyl rings and the vinyl “rigid” fragments maintain a fixed structure as they rotate relative to each other. Each ring was assumed to have  $C_{2v}$  symmetry, and it therefore requires a couple of interaction parameters  $\varepsilon_{2,0}^R$  and  $\varepsilon_{2,2}^R$ , whereas the vinyl group, assumed as effectively represented by an axially symmetric interaction tensor, needs just one independent element  $\varepsilon_{2,0}^{(H_6-C=C-H_7)}$ , the component along the  $C=C$  bond direction. Then, we tried to reproduce the whole set of  $D_{ij}^{obs}$  (Table 1 of the paper), starting with the geometries of the fragments given in the Appendix and simultaneously adjusting (in a iterative way, by a nonlinear fitting program based on the gradients method),<sup>56</sup> the following parameters: the  $\varepsilon_{2,0}^R$ ,  $\varepsilon_{2,2}^R$  and  $\varepsilon_{2,0}^{(H_6-C=C-H_7)}$  interaction tensor parameters of eq 13; the  $\phi_1^M = \pm \phi_2^M$  angle, the  $h_1 = h_2$  value and the  $w_{(C_2)} = 1 - w_{(C_i)}$  weight of eq 11. This has been made in order to minimize the rms (root-mean-square) target function:

$$rms = \{M^{-1} \sum_{i < j} [D_{ij}(\text{observed}) - D_{ij}(\text{calculated})]^2\}^{1/2} \quad (16)$$

being  $M$  the number of independent couplings. It is worth emphasizing that  $\phi_1^M$ ,  $h_1$ , and  $w_{(C_2)}$  can be varied independently, but with the constraint that  $p_{iso}(\phi_1, \phi_2)$  of eq 11 is normalized (in particular, because of the molecular symmetry, we normalized the distribution function for  $-45^\circ \leq \phi_1 \leq 45^\circ$  and  $-45^\circ \leq \phi_2 \leq 45^\circ$ ). By the optimized values of iteration parameters (reported in Table 2) and by a slight refining of the vinyl geometries (see Table 3 in the Appendix) we were finally successful in reproducing the observed direct couplings with a low, very satisfactory rms of 1.67 Hz (the single dipolar couplings  $D_{ij}^{AP-DPD}$  calculated by this approach are reported, for comparison, in the last column of Table 1).

The surface  $p_{iso}(\phi_1, \phi_2)$ , resulting from the procedure described above, and the corresponding contour plot are shown in Figure 4. The main feature of the obtained  $p_{iso}(\phi_1, \phi_2)$  function is certainly represented by the existence of four symmetry related maxima of the probability function, corresponding to the  $C_2$  (absolute maxima) and  $C_i$  (relative maxima)

**Table 2.** Optimized Values of the Iteration Parameters Required by the AP-DPD Approach

$t$ -St in ZLI1132	
$\phi_1^M = \pm \phi_2^M/\text{deg}$	$16.80 \pm 0.02$
$h_1 = h_2/\text{deg}$	10 (after parametrization)
$w_{(C_2)}$	$0.59 \pm 0.01$
$\varepsilon_{2,0}^R/\text{kJ mol}^{-1}$	$0.473 \pm 0.002$
$\varepsilon_{2,2}^R/\text{kJ mol}^{-1}$	$1.349 \pm 0.001$
$\varepsilon_{2,0}^{(H_6-C=C-H_7)}/\text{kJ mol}^{-1}$	$1.593 \pm 0.006$

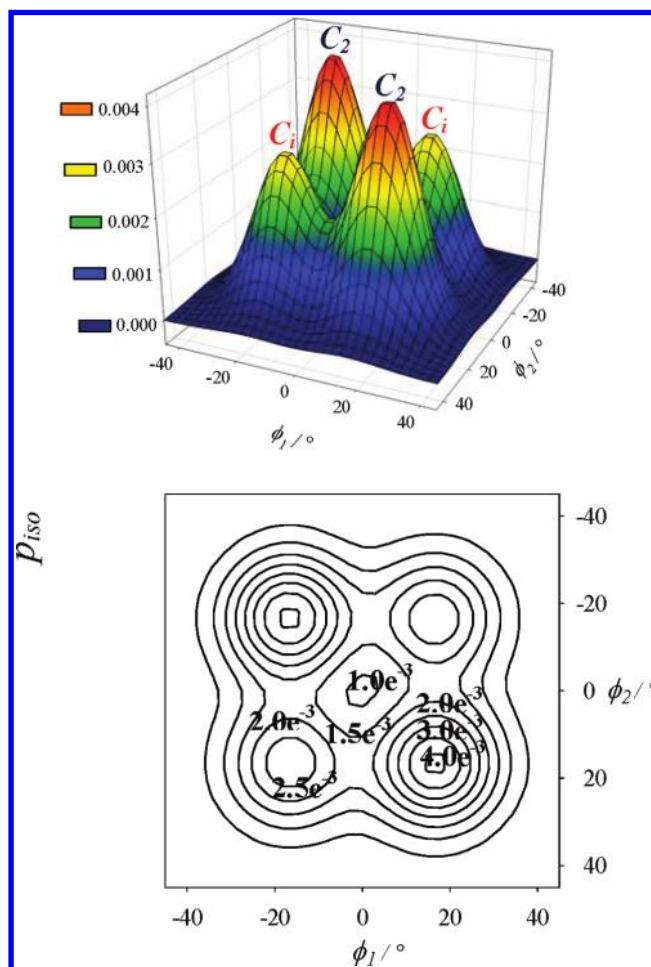


**Figure 4.** Experimental probability distribution  $p_{iso}(\phi_1, \phi_2)$  for  $t$ -St dissolved in the nematic solvent ZLI1132 at 298 K, obtained by the LXNMR conformational analysis (both, the 3D surface and its contour plot, are shown for the sake of clarity).

structures characterized by having, respectively,  $\phi_1^M = \phi_2^M$  and  $\phi_1^M = -\phi_2^M$ , with  $\phi_1^M = 16.8^\circ$  (see Table 2).

Finally, even though this paper is not aimed at determining the orientational ordering of  $t$ -St in liquid crystals, for the interested readers we report the  $S$  matrices of the stable rotamers of the molecule dissolved in ZLI1132 at 298 K. For the  $C_2$  conformation, the order parameters given in the Principal Axis System (PAS) of the Saupe matrix are the following (see Figure 3 for the definition of the molecular axes and of the  $\eta$  angle, giving the location of the PAS):  $S_{cc} = 0.525$  and  $S_{aa} - S_{bb} = 0.174$ , with  $\eta = 44.92^\circ$ . In the same molecular frame (the  $S$  PAS of  $C_2$ ) we also give the  $C_i$  order parameters:  $S_{cc} = 0.506$ ,  $S_{aa} - S_{bb} = 0.176$ ,  $S_{ab} = \pm 0.055$ ,  $S_{ac} \sim 0.0$  and  $S_{bc} = \mp 0.029$  (the  $\pm$  and  $\mp$  signs are of course referred to the two possible forms of  $C_i$ , namely  $\{\phi_1^M = +16.8^\circ; \phi_2^M = -16.8^\circ\}$



and  $\{\phi_1^M = -16.8^\circ; \phi_2^M = +16.8^\circ\}$ . *A posteriori*, it is interesting to observe that the final values of  $S_{cc}$  and  $S_{aa} - S_{bb}$  are really very similar to the trial ones  $S_{cc} = 0.590$  and  $S_{aa} - S_{bb} = 0.134$  “guessed” by us (by trial and error) to analyze the experimental spectrum (see section 3 above).

## 5. QUANTUM CHEMICAL CALCULATIONS

In order to shed more light on the problem widely described above, we decided to carry out rather accurate theoretical calculations *in vacuo*, by using the MP2/6-31G\*\* method (fairly reliable for this kind of conformational problems)<sup>34</sup> to determine the minima on the conformational potential energy surface (PES) for *t*-St (we also allowed for bond lengths and angles relaxation of the structure every  $3^\circ$  torsional steps). The calculations were performed using the Gaussian 03 (rev. C.02) software package<sup>57</sup> and required 17 days, 17 h and 15 min of CPU time on a server IBM e326, equipped with two processors AMD Opteron 2.6 GHz and 2GB of RAM (O.S.: SUSE Linux Enterprise Server 9 for AMD64). The obtained conformational PES is shown in Figure 5,

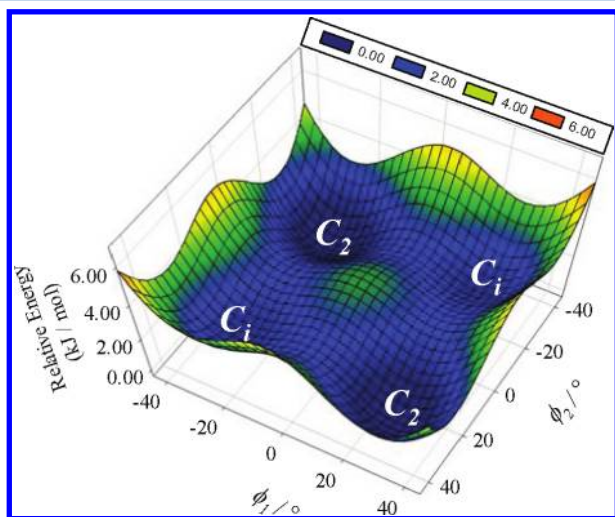


**Figure 5.** The conformational potential energy surface (PES) obtained for *trans*-stilbene from MP2/6-31G\*\* calculations. The locations of absolute and relative minima are labeled by means of their point group symbols (see text for more details).

where the presence of two global and two local minima is clearly evident (the significant geometrical parameters for the molecule in its more stable conformation are given in Table 3 of the Appendix).

The resulting absolute minima ( $C_2$  structures, where the relative torsional energy (RTE) is, of course, fixed to be 0 kJ/mol) and the relative minima ( $C_i$  structures corresponding to a RTE  $\sim 1.2$  kJ/mol) are characterized by having, respectively,  $\phi_1^m = \phi_2^m$  and  $\phi_1^m = -\phi_2^m$ , with  $\phi_1^m = 27^\circ$ . The  $C_{2h}$  planar conformation ( $\phi_1 = \phi_2 = 0^\circ$ ) is neither a minimum nor a saddle point, but rather a local maximum corresponding to a RTE of about 3 kJ/mol (anyway, it is worthwhile to emphasize that the just quoted values of energy could be more or less affected by the ZPVE corrections).<sup>34</sup> Even though, as said in the Introduction, the past literature witnesses that different theoretical approaches can give quite different results, it should be noticed that something very similar to what we have found here has been already obtained by another method;<sup>31</sup> this increases, in our opinion, the reliability of our findings. In order to make more effective and immediate the comparison between the just described theoretical results, referred to the isolated molecule, and the experimental LXNMR results in solution, we decided to

plot the probability resulting from the *ab initio* calculations as a function of  $\phi_1$  and  $\phi_2$ . The theoretical probability distribution  $p_{theo}$  (normalized for  $-45^\circ \leq \phi_1 \leq 45^\circ$  and  $-45^\circ \leq \phi_2 \leq 45^\circ$ ) is shown in Figure 6, where both the 3D and the contour plots of the function are given for more clarity.

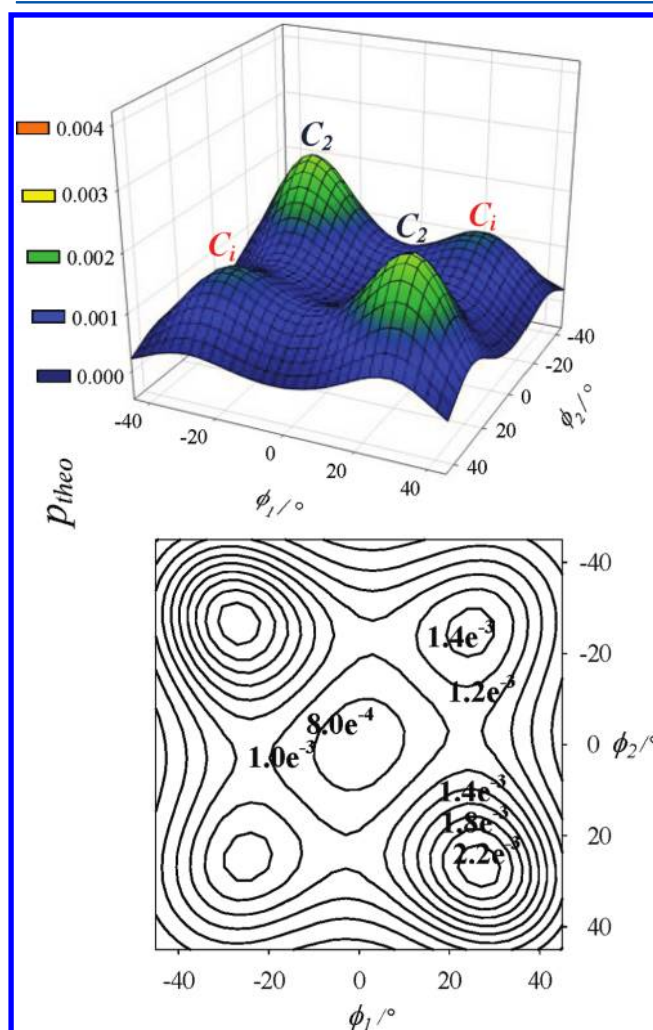


**Figure 6.** Normalized probability distribution  $p_{theo}$  for *trans*-stilbene, obtained from the theoretical PES of Figure 5.

## 6. COMPARISON BETWEEN *IN VACUO* THEORETICAL CALCULATIONS AND EXPERIMENTAL RESULTS IN SOLUTION

As interestingly anticipated in section 3, the basic non planarity of the molecule in solution had been qualitatively guessed, in a “model-free” way, from the simple appearance of the experimental LXNMR spectrum. Now, in the light of our final results, we observe that both the investigations carried out in this work manifestly agree in indicating non planar structures as the more stable conformations for the molecule. More in detail, a glance at Figure 4 and Figure 6 immediately reveals significant similarities, but also important differences, between the conformational probability distributions obtained from the two different treatments applied in this work. The similarities consist, of course, in the presence of the peculiar four “peaks” of probability belonging to the same symmetries (the two  $C_2$  global and the two  $C_i$  local maxima). The differences are in the

precise locations of the maxima and in their different heights. It is not possible to discern with certainty to which extent the differences are physically sensible or, on the contrary, whether the obtained results are deeply biased by the adopted methods of investigation of the torsional equilibrium. Reasoning within the more interesting hypothesis of real physical effects, we think that, all things considered, the fact that in solution the twist angles are smaller than those theoretically predicted *in vacuo* should not surprise us. As a matter of fact, in the above cited gas phase experimental study of ref 25 (whose issues can be quite safely compared with our theoretical results, both concerning the isolated *t*-St), the molecule was recognized to be basically a  $C_2$  structure with a twist angle of about  $32.5^\circ$ , not very dissimilar from our calculated  $27^\circ$ . Then, it seems that the intermolecular interactions, absent for the isolated molecule, contribute to force the molecule toward a less twisted arrangement (following this argument, it can be useful to recall here that the *t*-St is practically planar in its solid phase). This behavior is quite usual in conjugated systems as, for example, biphenyl (see ref 41 and references therein). Finally, our calculations say that the isolated molecule is “less confined” in the  $C_2$  and  $C_i$  high probability conformations with respect to the liquid state, where the probability peaks are higher and, of course, sharper. Nonetheless, a crude ratio between the probabilities exactly corresponding to  $C_2$  and  $C_i$  structures (given in the contour plots of Figures 4 and 6) roughly indicates relative percentages to be about 62% of  $C_2$  against 38% of  $C_i$  both in liquid and in gas phase.

## 7. CONCLUSIONS

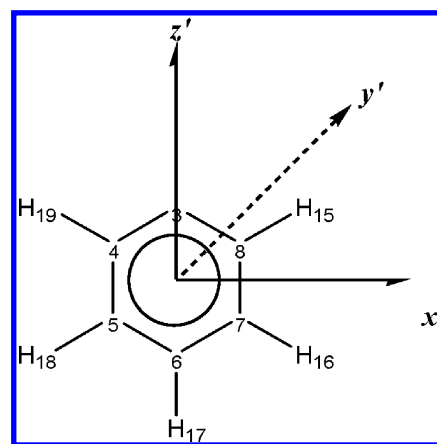
A basically non planar arrangement of *trans*-stilbene quite clearly emerges from our theoretical results *in vacuo* and from experimental outcomes in solution. This evidently means that the differences between the conformational behavior of the molecule in solution (where inter- and intramolecular forces act), with respect to the calculations on the isolated molecule (where, on the contrary, only intramolecular interactions are considered), are not enough to cancel the main features of the torsional probability distribution. As a matter of fact, four more stable conformations, two by two symmetry related (represented by a couple of global minima, where the molecule exhibits a propeller-like  $C_2$  symmetry, and a couple of  $C_i$  local minima, where the rings are “conrotated” of the same angle) have been found both for the molecule *in vacuo* (via the reliable MP2/6-31G\*\* theoretical calculations) and in solution (by the well tested experimental method of LXNMR conformational analysis). Of course, the probability distributions in the two phases are not identical, but the differences can be quite reasonably rationalized and explained. On the other hand, the calculated torsional potential of *t*-St (Figure 5) shows low barriers, comparable with  $k_B T$  at room temperature. This has at least a couple of relevant consequences: (1) since the preference for one or the other conformation is relatively weak, the system needs to be described in terms of the full torsional distribution (in other words: at room temperature  $C_2$  and  $C_i$  conformations are simultaneously present, and also the planar conformations are not totally absent); (2) the small energy differences may be one reason for the discrepancies between the results of different experiments (small changes of the experimental conditions, as the temperature and/or the solvent, might significantly affect the torsional distribution) and for the discrepancies between theoretical calculations performed at different levels (standard quantum chemical

calculations are not able to provide very reliable estimates of such small energy differences between minima). Given the great importance of *t*-St as a prototype molecule of many different compounds with innumerable properties (see the Introduction), we hope that our results, interesting, in our opinion, from a fundamental research point of view, can also contribute to a better understanding of useful structure–property relationships.

## ■ APPENDIX

### Molecular Geometry of *trans*-Stilbene

Assuming, as usually done in literature,<sup>44a,48</sup> that the structures of the sub-units making up the flexible molecule (and rotating relative to each other) are “rigid”, we can determine the fragment structures (independently from each other) from the whole set of observed interproton dipolar couplings obtained from the  $^1\text{H}$ -LXNMR spectrum of *t*-St dissolved in ZLI1132 (Table 1 of the work). It is worth recalling here that, from the proton NMR spectrum, we cannot of course have direct information about the carbon geometries of the molecule; so, only a “virtual” skeleton of the molecule can be hypothesized and assumed, compatible with the proton coordinates able to reproduce the observed  $D_{ij}^{obs}$ .



### Phenyl Rings Structure

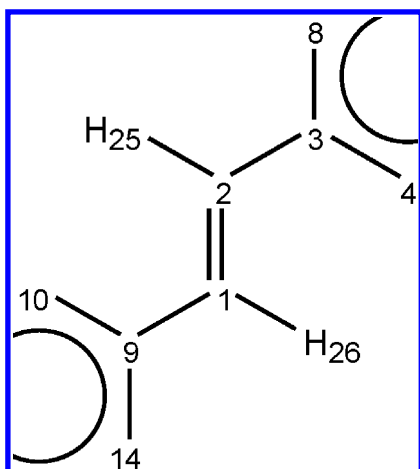
We have a total set of 6 intraring  $D_{ij}^{Ring(obs)}$  values (of course, the two ring sub-units in the molecule have been assumed to be structurally identical). First of all, we fixed the proton coordinates correspondingly to an “all- $120^\circ$ ” virtual (about what we mean with this word, see above) regular hexagon with  $\overline{CC} = 1.40 \text{ \AA}$  and  $\overline{CH} = 1.09 \text{ \AA}$ : this implies for the rings a  $C_{2v}$  local symmetry (consistent with the nuclear spin symmetry). Then, we adjusted the local order parameters  $S_{zz'}^{Ring}$ ,  $(S_{x'x'} - S_{y'y'})^{Ring}$ , and the  $C_7\hat{C}_8H_{15}$  angle (of course also the  $C_5\hat{C}_4H_{19}$  angle, equal to  $C_7\hat{C}_8H_{15}$ , has been correspondingly changed to keep the  $C_{2v}$  symmetry of the rings) in order to reproduce the 6 intraring dipolar couplings (3 degrees of freedom *versus* 6 experimental data mathematically represent a good overdetermination of the system). The final results were the following:  $C_7\hat{C}_8H_{15} = 119.25^\circ$ ;  $S_{zz'}^{Ring} = 0.5068$  and  $(S_{x'x'} - S_{y'y'})^{Ring} = 0.1754$ . These ring geometries were then kept fixed in all subsequent calculations.

### Structure of the Vinyl Fragment

Since only one local direct coupling is experimentally available for the *ene* fragment (the  $D_{25,26}^{obs}$  coupling constant), we were forced to start by borrowing the virtual geometries of this sub-unit from the theoretical calculations carried out by the



MP2/6-31G\*\* method (see text); then, during the LXNMR calculations, we slightly refined the initial geometries in order



to better reproduce the whole set of the observed couplings. As reported below (Table 3), the starting and refined values are fortunately very similar, so that, in our opinion, the used geometries can be considered reliable.

**Table 3. Starting and Refined Geometries of the Ene Group**

geometrical parameter	initial value (from MP2/6-31G** theoretical calculations)	refined value
$r_{1,2}$ / Å	1.352	1.337
$r_{2,3}$ / Å	1.466	1.477
$C_1\hat{C}_2C_3/\text{deg}$	124.83	125.54
$C_2\hat{C}_3C_4/\text{deg}$	120.80	122.49
$C_1\hat{C}_2H_{25}/\text{deg} = C_2\hat{C}_1H_{26}/\text{deg}$	118.78	120.24

## AUTHOR INFORMATION

### Corresponding Author

\*E-mail: giorgio.celebre@unical.it. Telephone: +39-0984493321. Fax: +39-0984493301.

### Notes

The authors declare no competing financial interest.

## ACKNOWLEDGMENTS

The present work has been supported by the European Commission, the European Social Fund, and the Regione Calabria through the cofunded Ph.D. scholarship of M.E.D.P. Moreover, the authors thank University of Calabria and MIUR PRIN 2009 for financial support. Finally, the authors wish to express indebtedness to an unknown reviewer for careful reading and valuable suggestions and comments, some of which have been introduced in the paper.

## REFERENCES

- (1) (a) Belluti, F.; Fontana, G.; Dal Bo, L.; Carenini, N.; Giommarelli, C.; Zunino, F. *Bioorgan. Med. Chem.* **2010**, *18*, 3543–3550. and refs therein (b) Frémont, L. *Life Sci.* **2000**, *66*, 663–673. (c) Matsuda, H.; Tomohiro, N.; Hiraba, K.; Harima, S.; Ko, S.; Matsuo, K.; Yoshikawa, M.; Kubo, M. *Biol. Pharm. Bull.* **2001**, *24*, 264–267.
- (2) (a) Savio, M.; Coppa, T.; Bianchi, L.; Vannini, V.; Maga, G.; Forti, L.; Cazzalini, O.; Lazzè, M. C.; Perucca, P.; Prosperi, E.; Stivala, L. A. *Int. J. Biochem. Cell B.* **2009**, *41*, 2493–2502. (b) Queiroz, A. N.;

Gomes, B. A. Q.; Moraes, W. M. Jr.; Borges, R. S. *Eur. J. Med. Chem.* **2009**, *44*, 1644–1649.

(3) (a) Heynekamp, J. J.; Weber, W. M.; Hunsaker, L. A.; Gonzales, A. M.; Orlando, R. A.; Deck, L. M.; Van der Jagt, D. L. *J. Med. Chem.* **2006**, *49*, 7182–7189. and refs therein (b) Kim, S.; Min, S. Y.; Lee, S. K.; Cho, W. J. *Chem. Pharm. Bull.* **2003**, *51*, S16–S21.

(4) (a) Bhat, K. P. L.; Lantvit, D.; Christov, K.; Mehta, R. G.; Moon, R. C.; Pezzuto, J. M. *Cancer Res.* **2001**, *61*, 7456–7463. (b) Korach, K. S.; Metzler, M.; McLachlan, J. A. *Proc. Natl. Acad. Sci. U.S.A.* **1978**, *75*, 468–471.

(5) Ko, S. K.; Lee, S. M.; Whang, W. K. *Arch. Pharm. Res.* **1999**, *22*, 401–403.

(6) (a) Hong, M. C.; Kim, Y. K.; Choi, J. Y.; Yang, S. Q.; Rhee, H.; Ryu, Y. H.; Choi, T. H.; Cheon, G. J.; An, G. I.; Kim, H. Y.; Kim, Y.; Kim, D. J.; Lee, J.-S.; Chang, Y.-T.; Lee, K. C. *Bioorgan. Med. Chem.* **2010**, *18*, 7724–7730. (b) Chen, X. J. *Mol. Struct.—THEOCHEM.* **2006**, *763*, 83–89.

(7) (a) Rotta, R.; Neto, Á. C.; de Lima, D. P.; Beatriz, A.; da Silva, G. V. J. *J. Mol. Struct.* **2010**, *975*, 59–62. (b) Aslam, S. N.; Stevenson, P. C.; Kokubun, T.; Hall, D. R. *Microbiol. Res.* **2009**, *164*, 191–195.

(8) (a) Ravikrishnan, A.; Sudhakara, P.; Kannan, P. J. *Mater. Sci.* **2010**, *45*, 435–442. (b) Buathong, S.; Gehringer, L.; Donnio, B.; Guillon, D. C. R. *Chim.* **2009**, *12*, 138–162.

(9) Zoppi, L.; Calzolari, A.; Ruini, A.; Ferretti, A.; Caldas, M. J. *Phys. Rev. B* **2008**, *78*, 165204.

(10) Papper, V.; Likhtenshtein, G. I. *J. Photochem. Photobiol. A* **2001**, *140*, 39–52 and refs. therein.

(11) Buruiana, E. C.; Zamfir, M.; Buruiana, T. *Eur. Polym. J.* **2007**, *43*, 4316–4324.

(12) (a) Tomatsu, I.; Peng, K.; Kros, A. *Adv. Drug Delivery Rev.* **2011**, *63*, 1257–1266. (b) Meng, F.; Zhong, Z.; Feijen, J. *Biomacromolecules* **2009**, *10*, 197–209.

(13) Finder, C. J.; Newton, M. G.; Allinger, N. L. *Acta Crystallogr.* **1974**, *B30*, 411–415.

(14) Bernstein, J. *Acta Crystallogr.* **1975**, *B31*, 1268–1271.

(15) Tachon, M.; Davies, E.; Lamotte, M.; Muszkat, K. A.; Wisniewski-Kittel, T. J. *Phys. Chem.* **1994**, *98*, 11870–11877.

(16) Myers, A. B.; Trulson, M. O.; Mathies, R. A. *J. Chem. Phys.* **1985**, *83*, 5000–5006.

(17) Suzuki, T.; Mikami, N.; Ito, M. *J. Phys. Chem.* **1986**, *90*, 6431–6440.

(18) Baskin, J. S.; Felker, P. M.; Zewail, A. H. *J. Chem. Phys.* **1987**, *86*, 2483–2499.

(19) Spangler, L. H.; v. Zee, R.; Zwier, T. S. *J. Phys. Chem.* **1987**, *91*, 2782–2786.

(20) Spangler, L. H.; v. Zee, R.; Blankespoor, S. C.; Zwier, T. S. *J. Phys. Chem.* **1987**, *91*, 6077–6079.

(21) Baskin, J. S.; Zewail, A. H. *J. Phys. Chem.* **1989**, *93*, 5701–5717.

(22) Champagne, B. B.; Pfanstiel, J. F.; Plusquellic, D. F.; Pratt, D. W.; van Herpen, W. M.; Meerts, W. L. *J. Phys. Chem.* **1990**, *94*, 6–8.

(23) Chiang, W.-Y.; Laane, J. J. *J. Chem. Phys.* **1994**, *100*, 8755–8767.

(24) Syage, J. A.; Felker, P. M.; Zewail, A. H. *J. Chem. Phys.* **1984**, *81*, 4685–4640.

(25) Traetteberg, M.; Frantsen, E. B.; Mijlthoff, F. C.; Hoekstra, A. *J. Mol. Struct.* **1975**, *26*, 57–68.

(26) Maier, J. P.; Turner, D. W. *J. Chem. Soc., Faraday Trans. 2* **1973**, *54*, 196–206.

(27) Rademacher, P.; Marzinzik, A. L.; Kowski, K.; Weiß, M. E. *J. Org. Chem.* **2001**, 121–130.

(28) Chen, P. C.; Chieh, Y. C. *J. Mol. Struct.—THEOCHEM.* **2003**, *624*, 191–200 and references therein.

(29) Kwasniewski, S. P.; Claes, L.; François, J.-P.; Deleuze, M. S. *J. Chem. Phys.* **2003**, *118*, 7823–7836 and references therein.

(30) Quenneville, J.; Martínez, T. J. *J. Chem. Phys. A* **2003**, *107*, 829–837.

(31) Freile, M. L.; Risso, S.; Curaqueso, A.; Zamora, M. A.; Enriz, R. D. *J. Mol. Struct.—THEOCHEM.* **2005**, *731*, 107–114.

(32) Vendrame, R.; Coluci, V. R.; Galvão, D. S. *J. Mol. Struct.—THEOCHEM.* **2004**, *686*, 103–108.

- (33) Catalán, J. *Chem. Phys. Lett.* **2006**, *421*, 134–137.
- (34) Chowdary, P. D.; Martinez, T. J.; Gruebele, M. *Chem. Phys. Lett.* **2007**, *440*, 7–11.
- (35) Bree, A.; Edelson, M. *Chem. Phys.* **1980**, *51*, 77–88.
- (36) Novak, P.; Meić, Z.; Sterk, H. *J. Chem. Soc., Perkin Trans. 2* **1996**, *11*, 2531–2536.
- (37) Choi, C. H.; Kertesz, M. *J. Phys. Chem. A* **1997**, *101*, 3823–3831.
- (38) Furuya, K.; Kawato, K.; Yokoyama, H.; Sakamoto, A.; Tasumi, M. *J. Phys. Chem. A* **2003**, *107*, 8251–8258.
- (39) Celebre, G.; De Luca, G.; Longeri, M.; Emsley, J. W. *Mol. Phys.* **1989**, *67*, 239–248 and references therein.
- (40) Celebre, G.; De Luca, G.; Longeri, M.; Ferrarini, A. *Mol. Phys.* **1994**, *83*, 309–326 and references therein.
- (41) Celebre, G.; De Luca, G.; Longeri, M. *Liq. Cryst.* **2010**, *37*, 923–933.
- (42) Celebre, G.; De Luca, G.; Longeri, M.; Sicilia, E. *J. Chem. Inf. Comput. Sci.* **1994**, *34*, 539–545.
- (43) Diehl, P. in *Nuclear Magnetic Resonance of Liquid Crystals*; Emsley, J. W., Ed.; Reidel: Dordrecht, The Netherlands, 1985; pp 147–180 and references therein.
- (44) (a) Celebre, G.; Longeri, M. In *NMR of Ordered Liquids*; Burnell, E. E., de Lange, C. A., Eds.; Kluwer: Dordrecht, The Netherlands, 2003; pp 305–324. (b) The director aligns parallel or perpendicular to  $B_0$ , depending on the sign of solvent diamagnetic susceptibility anisotropy  $\Delta\chi = \chi_{\parallel} - \chi_{\perp}$  (in particular,  $\Delta\chi > 0$ , parallel arrangement;  $\Delta\chi < 0$ , perpendicular arrangement): de Gennes, P. G.; Prost, J. *The Physics of Liquid Crystals*; Oxford Science: London, 1993.
- (45) Emsley, J. W.; Luckhurst, G. R.; Stockley, C. P. *Proc. R. Soc. London, Ser. A* **1982**, *381*, 117–138.
- (46) Emsley, J. W. in *Encyclopedia of NMR*, Eds. Grant, D. M. Harris, R. K., J. Wiley & Sons Ltd: Chichester, 1996; pp 2781–2787.
- (47) Celebre, G.; De Luca, G.; Emsley, J. W.; Foord, E. K.; Longeri, M.; Lucchesini, F.; Pileio, G. *J. Chem. Phys.* **2003**, *118*, 6417–6426.
- (48) Celebre, G.; De Luca, G.; Longeri, M.; Pileio, G.; Emsley, J. W. *J. Chem. Phys.* **2004**, *120*, 7075–7084.
- (49) Celebre, G.; Concistrè, M.; De Luca, G.; Longeri, M.; Pileio, G.; Emsley, J. W. *Chem.—Eur. J.* **2005**, *11*, 3599–3608.
- (50) Concistrè, M.; De Lorenzo, L.; De Luca, G.; Longeri, M.; Pileio, G.; Raos, G. *J. Phys. Chem. A* **2005**, *109*, 9953–9963.
- (51) Celebre, G.; Cinacchi, G. *J. Chem. Phys.* **2006**, *124*, 176101 and references therein.
- (52) Celebre, G.; Concistrè, M.; De Luca, G.; Longeri, M.; Pileio, G. *Chem. Phys. Chem.* **2006**, *7*, 1930–1943.
- (53) Emsley, J. W.; De Luca, G.; Lesage, A.; Merlet, D.; Pileio, G. *Liq. Cryst.* **2007**, *34*, 1071–1093.
- (54) Emsley, J. W.; Lesot, P.; De Luca, G.; Lesage, A.; Merlet, D.; Pileio, G. *Liq. Cryst.* **2008**, *35*, 443–464.
- (55) Brink, D. M.; Satchler, G. R., *Angular Momentum*, 3rd ed., Clarendon Press: Oxford, U.K., 1993.
- (56) Schlegel, H. B. *J. Comput. Chem.* **1982**, *3*, 214–218.
- (57) Gaussian 03, Revision C.02, Frisch, M. J.; Trucks, G. W.; Schlegel, H. B.; Scuseria, G. E.; Robb, M. A.; Cheeseman, J. R.; Montgomery, J. A., Jr.; Vreven, T.; Kudin, K. N.; Burant, J. C.; Millam, J. M.; Iyengar, S. S.; Tomasi, J.; Barone, V.; Mennucci, B.; Cossi, M.; Scalmani, G.; Rega, N.; Petersson, G. A.; Nakatsuji, H.; Hada, M.; Ehara, M.; Toyota, K.; Fukuda, R.; Hasegawa, J.; Ishida, M.; Nakajima, T.; Honda, Y.; Kitao, O.; Nakai, H.; Klene, M.; Li, X.; Knox, J. E.; Hratchian, H. P.; Cross, J. B.; Adamo, C.; Jaramillo, J.; Gomperts, R.; Stratmann, R. E.; Yazyev, O.; Austin, A. J.; Cammi, R.; Pomelli, C.; Ochterski, J. W.; Ayala, P. Y.; Morokuma, K.; Voth, G. A.; Salvador, P.; Dannenberg, J. J.; Zakrzewski, V. G.; Dapprich, S.; Daniels, A. D.; Strain, M. C.; Farkas, O.; Malick, D. K.; Rabuck, A. D.; Raghavachari, K.; Foresman, J. B.; Ortiz, J. V.; Cui, Q.; Baboul, A. G.; Clifford, S.; Cioslowski, J.; Stefanov, B. B.; Liu, G.; Liashenko, A.; Piskorz, P.; Komaromi, I.; Martin, R. L.; Fox, D. J.; Keith, T.; Al-Laham, M. A.; Peng, C. Y.; Nanayakkara, A.; Challacombe, M.; Gill, P. M. W.; Johnson, B.; Chen, W.; Wong, M. W.; Gonzalez, C.; Pople, J. A.; Gaussian, Inc.: Pittsburgh PA, 2003.